First Principles Examination of the Acetylene−Water Clusters, HCCH−(H2O)x, x = 2, 3, and 4

ARTICLE *in* THE JOURNAL OF PHYSICAL CHEMISTRY A · OCTOBER 2002

Impact Factor: 2.69 · DOI: 10.1021/jp021191q

2 AUTHORS:

Demeter Tzeli
National Hellenic Research Foundation
52 PUBLICATIONS **505** CITATIONS
SEE PROFILE

Aristides Mavridis
National and Kapodistrian University of Athens
137 PUBLICATIONS **1,673** CITATIONS
SEE PROFILE

First Principles Examination of the Acetylene−Water Clusters, HCCH−$(H_2O)_x$, $x = 2$, 3, and 4

Demeter Tzeli and Aristides Mavridis*

Laboratory of Physical Chemistry, Department of Chemistry, National and Kapodistrian University of Athens, P.O. Box 64 004, 157 10 Zografou, Athens, Greece

Sotiris S. Xantheas

Environmental Molecular Sciences Laboratory, Pacific Northwest National Laboratory, 906 Battelle Boulevard, P.O. Box 999, MS K8-91, Richland, Washington 99352

Received: May 13, 2002; In Final Form: September 3, 2002

The acetylene−water (A−W) interactions have been investigated by examining the van der Waals clusters AW_x, $x = 2$, 3, and 4, at the second order (MP2) perturbation theory using the correlation-consistent basis sets, aug-cc-pV*n*Z, $n = D$ (AW_2, AW_3, and AW_4), T (AW_2). We located 4 minima (m) and 2 saddle points (sp), 10 m and 3 sp, and 30 m and 3 sp on the potential energy surfaces of the AW_2, AW_3, and AW_4 clusters, respectively. We report the fully optimized geometries and interaction energies ΔE_e, including corrections for basis set superposition error, ΔE_e(BSSE), as well as zero-point energies, ΔE_0(BSSE), for the various stationary points. The global minima of the AW_2 and AW_3 clusters are cyclic configurations in which the acetylene molecule inserts into the water hydrogen bonding network. The corresponding interaction energies ΔE_e(BSSE)[ΔE_0(BSSE)] are AW_2, −10.37 [−6.70] kcal/mol (MP2/aug-cc-pVTZ) and AW_3, −17.80 [−11.46] kcal/mol (MP2/aug-cc-pVDZ). The global minimum of AW_4 corresponds to a van der Waals complex between a cyclic water tetramer W_4 and A with an interaction energy of −28.01 [−18.67] kcal/mol (MP2/aug-cc-pVDZ). The 4 and 10 local minima for the $x = 2$ and 3 clusters span an energy range of 4.3 and 6.1 kcal/mol above the respective global minima. For AW_4, the energy range for the 30 minima is 14.1 kcal/mol; however, the first 28 lie within 8.4 kcal/mol above the global minimum. The analysis of the many-body interaction energy terms suggests that the global and low-lying ring networks are stabilized by the maximization of the many-body (mainly the 3-body) terms, whereas the higher lying minima are mainly described by 2-body interactions.

1. Introduction

The present work is a continuation of our study on the aqueous microsolvation of acetylene.[1,2] In the first paper,[1] we presented an extensive study of the potential energy surface (PES) of the C_2H_2−H_2O (acetylene-water, AW) dimer, where two minima, a global AW−Y (the water acting as proton acceptor), a local AW−T (the water acting as proton donor), and three transition states (shown in Figure 1) were located. However, because of basis set superposition errors (BSSE) and zero-point energy (ZPE) corrections, the AW−T local minimum is destabilized, and it can "slip" into the global minimum (AW−Y), thus explaining the experimental observation of a single isomer.[3−5] In a subsequent paper,[2] we identified the spectroscopic signature for the predicted change in the structural pattern between AW_3 and AW_4 from a cyclic configuration that incorporates acetylene (A) into the water hydrogen bonding network (AW_3) to a van der Waals complex between A and a cyclic water tetramer (AW_4). That study also produced qualitative differences between the ab initio results and those with an empirical potential as regards the structures of the global minima of the first few AW_x clusters.

To the best of our knowledge, there currently exists limited experimental and/or theoretical work on acetylene−water clusters (AW_x, $x > 1$).[6−8] Besides our previous work,[2] we are aware of only three publications on the AW_x clusters. Choi et al.[6] studied the ion/molecule reactions within the acetylene-water heterocluster ions $(C_2H_2)_n{\cdot}(H_2O)_m^+$ using electron impact time-of-flight mass spectrometry. Dykstra,[7] employing the molecular mechanics for clusters (MMC) model potential, calculated an interaction energy of $\Delta E_e = -12.65$ kcal/mol ($\Delta E_o = -8.17$ kcal/mol, including ZPE corrections) for AW_2. van Voorhis and Dykstra,[8] used the MMC model potential for AW_3, comparing it with a number of other four-membered water containing clusters. They found four local minima within 0.8 kcal/mol of their global minimum, with one of those only 0.24 kcal/mol higher. Their characterization of the global minimum has it much like W_3 with an adjacent acetylene. Our results show five local

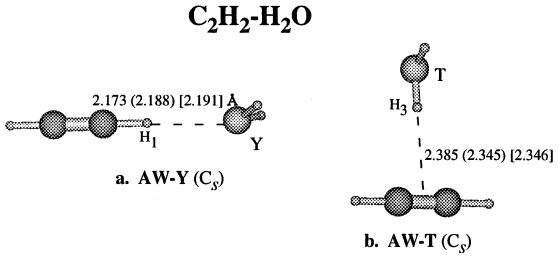

Figure 1. Geometries of the AW−Y and AW−T minima. Bond distances in Å at the MP2/avdz(avtz)[avqz] level.

* To whom correspondence should be addressed. E-mail: mavridis@chem.uoa.gr.

10.1021/jp021191q CCC: $22.00
Published on Web 10/24/2002

minima within 0.8 kcal/mol of the global minimum, but the global minimum is a four-membered ring, and the secondary minimum is 0.26 kcal/mol (0.37 kcal/mol including ZPE) higher in energy. The same authors refer also to a AW_4 minimum as a cyclic water tetramer interacting with acetylene but without reporting any structural or energetic results.

In view of the rich structural patterns found in the first few AW_x clusters and the disagreement between the earlier ab initio results and the ones obtained with empirical models, we have extended our previous work into a detail investigation of the global and local minima of the AW_x, $x = 2$, 3, and 4, clusters. The present investigation is organized as follows: in section 2, we outline the computational approach; in section 3, we report the structures and energetics of the various stationary points; and finally in section 4, we summarize our findings and main conclusions.

2. Computational Approach

A preliminary sampling of the configuration space and the different hydrogen bonding networks was performed with the smaller 4-31G basis set. The resulting geometries were used as starting points and were subsequently fully optimized with the augmented correlation consistent basis sets, aug-cc-pV*n*Z (=av*n*z), n = D and T, of Dunning and co-workers.[9] For AW_2, both the avdz and avtz sets were used, whereas the avdz set was employed for the AW_3 and AW_4 clusters. In some instances, configurations of higher symmetry were probed, and this resulted in obtaining saddle points (sp) of higher order (i.e., configurations for which the Hessian matrix has more than one negative eigenvalues). All calculations were performed at the second-order perturbation (MP2) level of theory with the Gaussian 98[10] programs. The "very tight" or "tight" options were used in all geometry optimizations. Energies were converged to about 0.01 μhartree, and the corresponding root-mean-square deviations of energy gradients with respect to nuclear coordinates were $\sim$11 μhartree/bohr. Harmonic vibrational frequencies were computed for all AW_2 and AW_3 minima and saddle points and for three minima for AW_4 at the MP2/avdz level. Furthermore, for the four AW_2 minima, the harmonic frequencies were also obtained with the avtz basis set.

Corrections due to basis set superposition error (BSSE),[11] which are important for weakly bound van der Waals complexes,[12] are taken into account following a procedure described earlier[13] and briefly outlined below.

The interaction energy $\Delta E_e(AW_x)$ of the AW_x cluster is defined as

$$\Delta E_e(AW_x) = E^{aw_x}_{AW_x}(AW_x) - E^{a}_{A}(A) - xE^{w}_{W}(W) \qquad (1)$$

where, $E^{s}_{G}(M)$ refers to the total energy of the molecule M at the geometry G, computed with basis set *s*; the above relation is modified appropriately when the BSSE correction is taken into account. For instance, the (BSSE)-corrected interaction energy, $\Delta E_e(BSSE)$, for the AW_4 cluster can be written as

$$\Delta E_e(BSSE) = E^{aw_4}_{AW_4}(AW_4) - E^{aw_4}_{AW_4}(A) - \sum_{i=a}^{d} E^{aw_4}_{AW_4}(W_i) + R_A + \sum_{i=a}^{d} R_{W_i}, \qquad (2)$$

where R are relaxation or deformation terms defined by the relations

$$R_A = E^{a}_{AW_x}(A) - E^{a}_{A}(A) \qquad (3a)$$

$$R_{W_i} = E^{w_i}_{AW_x}(W_i) - E^{w_i}_{W_i}(W_i),\ i = a, b, c, d \qquad (3b)$$

and W_i (i = a, b, c, and d) refers to the four water molecules, respectively.

Similarly, the analysis of the many-body interaction energy terms was performed using a procedure described before[14] which is based on casting the total energy of the n-body cluster $X_1X_2X_3...X_n$ as

$$E^{X_1X_2...}_{X_1X_2...}(X_1X_2...) = \sum_{i=1}^{n} E^{X_i}_{X_1X_2...}(X_i) + \sum_{i}^{n-1}\sum_{j>i}^{n} \Delta^2 E^{X_iX_j}_{X_1X_2...}(X_iX_j) + \sum_{i}^{n-2n-1}\sum_{j>i}^{n}\sum_{k>j} \Delta^3 E^{X_iX_j}_{X_1X_2...}(X_iX_j) + ... \qquad (4)$$

where Δ^2E, Δ^3E, ... are two-, three-, etc. body terms, respectively, defined as

$$\Delta^2 E^{X_iX_j}_{X_1X_2...}(X_iX_j) = E^{X_iX_j}_{X_1X_2...}(X_iX_j) - \{E^{X_i}_{X_1X_2...}(X_i) + E^{X_j}_{X_1X_2...}(X_j)\} \qquad (5)$$

$$\Delta^3 E^{X_iX_jX_k}_{X_1X_2...}(X_iX_jX_k) = E^{X_iX_jX_k}_{X_1X_2...}(X_iX_jX_k) - \{E^{X_i}_{X_1X_2...}(X_i) + E^{X_j}_{X_1X_2...}(X_j) + E^{X_k}_{X_1X_2...}(X_k)\} - \{\Delta^2 E^{X_iX_j}_{X_1X_2...}(X_iX_j) + \Delta^2 E^{X_iX_k}_{X_1X_2...}(X_iX_k) + \Delta^2 E^{X_jX_k}_{X_1X_2...}(X_jX_k)\} \qquad (6)$$

In the preceding, the one-, two-, three-, etc. body term summations contain $\binom{n}{1}$, $\binom{n}{2}$, $\binom{n}{3}$, ... terms, respectively, for a total of $\sum_{m=1}^{n}\binom{n}{m} = 2^n - 1$ terms.

In this notation, the BSSE-corrected, two- and three-body terms are[14b,c]

$$\Delta^2 E^{X_1X_2...}_{X_1X_2...}(X_iX_j,BSSE) = E^{X_1X_2...}_{X_1X_2...}(X_iX_j) - \{E^{X_1X_2...}_{X_1X_2...}(X_i) + E^{X_1X_2...}_{X_1X_2...}(X_j)\} \qquad (7)$$

$$\Delta^3 E^{X_1X_2...}_{X_1X_2...}(X_iX_jX_k,BSSE) = E^{X_1X_2...}_{X_1X_2...}(X_iX_jX_k) - \{E^{X_1X_2...}_{X_1X_2...}(X_i) + E^{X_1X_2...}_{X_1X_2...}(X_j) + E^{X_1X_2...}_{X_1X_2...}(X_k)\} - \{\Delta^2 E^{X_1X_2...}_{X_1X_2...}(X_iX_j) + \Delta^2 E^{X_1X_2...}_{X_1X_2...}(X_iX_k) + \Delta^2 E^{X_1X_2...}_{X_1X_2...}(X_jX_k)\} \qquad (8)$$

3. Results and Discussion

a. C_2H_2, H_2O, and $C_2H_2-H_2O$. For the purpose of analyzing our current data, we list the results of our previous work[1] on the $C_2H_2-H_2O$ cluster in Table 1. Specifically, the total and interaction energies of A, W, (AW−Y), (AW-T), W_x,[15] $x = 2$, 3, and 4, and selected optimal internal coordinates of (AW−Y) and (AW−T) at the MP2/av*n*z, n = D and T level of theory are listed (see Figure 1 for the corresponding structures). Table 1 contains a subset of the results of the exhaustive study of the PES of (AW) previously reported in ref 1.

b. C_2H_2 $(H_2O)_2$. We have located six stationary points, four minima (m), and two saddle points (sp) on the PES of AW_2; their structures are shown in Figure 2. The geometries of all six stationary points were fully optimized with the avdz basis set, whereas the four minima were also optimized with the larger avtz set.[16a] Their total energies (E_e), interaction energies with respect to the isolated fragments (ΔE_e), and BSSE-corrected

TABLE 1: Total Energies E_e (hartree), Interaction Energies ΔE_e (kcal/mol), Corrected for BSSE, ΔE_e(BSSE) (kcal/mol), and Harmonic ZPE, (kcal/mol), of C_2H_2, H_2O, $C_2H_2-H_2O$ (AW−Y, AW-T), and $(H_2O)_x$, $x = 2$, 3, and 4[a]

	avdz	avtz	avdz	avtz
	C_2H_2		H_2O	
E_e	−77.092997	−77.164058	−76.260909	−76.328992
ZPE	15.90	16.65	13.39	13.44
	$C_2H_2...H_2O$(AW−Y)[b]		$C_2H_2...H_2O$(AW-T)[b]	
R_{vdw} [d]	2.173	2.188[c]	2.385	2.345
ϕ_{vdw} [e]	171.1	155.8	178.5	177.5
E_e	−153.359654	−153.498094	−153.358758	−153.497859
ΔE_e	−3.61	−3.17	−3.04	−3.02
ΔE_e(BSSE)	−2.62	−2.72	−2.16	−2.56
ZPE	30.31	31.03	30.44	31.26

	avdz	avtz	avdz	avtz
	$(H_2O)_2$ [f]		$(H_2O)_3$ [f]	$(H_2O)_4$ [f]
E_e	−152.530207	−152.666241	−228.808800	−305.089433
ΔE_e	−5.26	−5.18	−16.36	−28.27
ΔE_e(BSSE)	−4.43	−4.71	−13.89	−24.37
ZPE	28.91	29.14	45.54	61.86

[a] van der Waals Geometries, R_{vdW}(Å) and ϕ_{vdW}(degrees) of AW−Y and AW−T clusters at the MP2/av*n*z, n = D and T level. [b] See Figure 1. [c] Experimental value 2.229 Å, ref 4. [d] H_1...O distance in AW−Y (Figure 1a), H_3...middle of the triple bond in AW-T (Figure 1b). [e] Angle between the C≡C and $C_2(H_2O)$ axes in AW−Y(Figure 1a); angle between O−H_3-middle of the triple bond in AW-T (Figure 1b). [f] References 13 and 15.

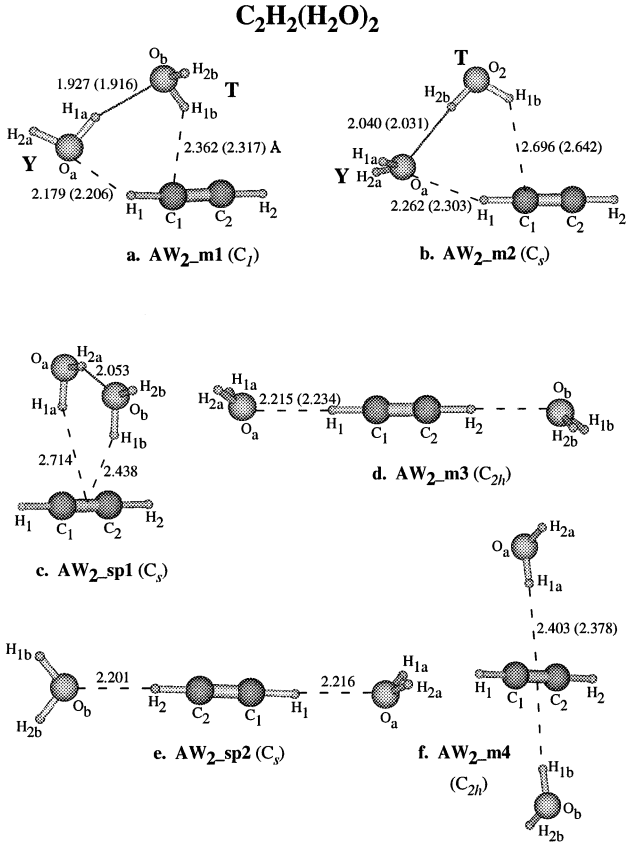

Figure 2. Geometries of the four minima (AW_2_m*n*, $n = 1-4$) and the two saddle points (AW_2_sp*n*, $n = 1-2$) of AW_2. Bond distances in Å at the MP2/avdz(avtz) level.

interaction energies, ΔE_e(BSSE) are listed in Table 2; van der Waals (vdW) intermolecular distances are also displayed in Figure 2. Harmonic vibrational frequencies and IR intensities of the global minimum are shown in Table 3.[16b] Finally, the decomposition of the interaction energy of the structures into many-body terms is reported in Table 4. Note that the minima and saddle points are ordered according to their uncorrected (for BSSE and ZPE) interaction energies (ΔE_e).

TABLE 2: Total Energies E_e (hartree), Interaction Energies ΔE_e (kcal/mol), Corrected for BSSE [ΔE_e(BSSE)], and Zero-Point Energy [ΔE_0(BSSE)] for the AW_2 Cluster at the MP2 Level with the avdz and avtz Basis Sets

AW_2 [a]	E_e	ΔE_e	ΔE_e(BSSE)	ΔE_0(BSSE)
		avdz		
m1	−229.633966	−12.02	−9.60	−5.76
m2	−229.629037	−8.92	−6.88	−3.71
sp1[b]	−229.627971	−8.25	−6.23	−3.57
m3	−229.625556	−6.74	−4.81	−2.71
sp2[c]	−229.625506	−6.71	−4.47	−2.47
m4	−229.623800	−5.64	−3.90	−1.75
		avtz		
m1	−229.840473	−11.57	−10.37	−6.70
m2	−229.835290	−8.31	−7.34	−4.37
m3	−229.831277	−5.79	−4.91	−3.03
m4	−229.830802	−5.50	−4.61	−2.45

[a] m(minimum) and sp (saddle point) according to Figure 2. [b] Two imaginary frequencies. [c] One imaginary frequency.

TABLE 3: Harmonic Vibrational Frequencies ω (cm^{-1}), IR Intensities IR−I (km/mol), and Zero-Point Energies ZPE (kcal/mol) of the Global Minima of AW_x, $x = 2$, 3, and 4 at the MP2 Level of Theory with the avdz and avtz (for AW_2) Basis Sets

	AW_2_m1			AW_3_m1		AW_4_m1	
	avdz		avtz	avdz		avdz	
	ω	IR−I	ω	ω	IR−I	ω	IR−I
ω_1	88	3.75	91	32	0.591	23	0.228
ω_2	94	18.1	95	57	3.06	39	0.211
ω_3	118	46.0	116	115	18.0	66	0.132
ω_4	148	30.2	151	122	2.79	80	1.83
ω_5	170	13.4	173	151	36.8	99	1.54
ω_6	183	88.2	192	163	8.00	122	4.24
ω_7	192	18.4	194	170	35.6	146	0.398
ω_8	240	69.7	251	191	95.9	198	2.50
ω_9	348	144	351	207	24.8	221	75.9
ω_{10}	467	38.6	495	236	21.2	237	15.5
ω_{11}	476	6.09	622	252	129	254	9.43
ω_{12}	530	42.3	636	283	65.4	264	86.5
ω_{13}	687	132	691	402	52.1	269	96.9
ω_{14}	775	105	804	418	22.3	285	144
ω_{15}	794	77.9	827	476	13.4	356	70.9
ω_{16}	1629	69.5	1634	490	29.0	413	3.50
ω_{17}	1644	28.7	1651	554	54.5	440	18.6
ω_{18}	1931	5.21	1952	729	119	452	37.7
ω_{19}	3363	228	3365	809	158	463	7.92
ω_{20}	3488	3.55	3497	821	95.2	479	6.28
ω_{21}	3647	285	3657	862	20.5	482	18.5
ω_{22}	3734	147	3741	1632	55.3	713	123
ω_{23}	3891	138	3901	1644	60.1	767	92.4
ω_{24}	3899	104	3910	1664	11.6	775	165
ω_{25}				1922	17.6	807	173
ω_{26}				3297	379	850	134
ω_{27}				3478	12.6	994	4.92
ω_{28}				3532	570	1639	84.6
ω_{29}				3581	534	1652	48.7
ω_{30}				3694	277	1661	80.6
ω_{31}				3883	142	1685	10.6
ω_{32}				3886	99.9	1934	3.97
ω_{33}				3894	88.7	3367	142
ω_{34}						3381	260
ω_{35}						3445	1378
ω_{36}						3484	633
ω_{37}						3493	7.41
ω_{38}						3591	393
ω_{39}						3832	129
ω_{40}						3881	92.5
ω_{41}						3882	84.9
ω_{42}						3885	84.0
ZPE	46.51		47.18	62.39		78.78	

TABLE 4: Many-Body Decomposition of the Interaction Energies (in kcal/mol) of the AW_2 at the MP2/avdz and avtz Levels of Theory[a]

AW_2 [b]	m1	m2	sp1	m3	sp2	m4
			avdz			
$A-W_a$	−2.94(−2.09)	−3.16(−2.40)	−2.48(−1.92)	−3.58(−2.64)	−3.59(−2.64)	−3.04(−2.19)
$A-W_b$	−3.00(−2.18)	−1.05(−0.46)	−2.56(−1.78)	−3.58(−2.64)	−2.98(−2.65)	−3.04(−2.19)
W_a-W_b	−5.20(−4.33)	−5.11(−4.39)	−3.36(−2.69)	0.00 (0.12)	0.17 (0.17)	0.15 (0.17)
total two body	−11.13(−8.60)	−9.32(−7.25)	−8.41(−6.38)	−7.17(−5.15)	−6.40(−5.13)	−5.93(−4.22)
A−W−W	−1.06(−1.18)	0.36(0.34)	0.07(0.07)	0.41(0.32)	−0.33 0.63)	0.29(0.31)
relaxation	0.18	0.03	0.08	0.02	0.02	0.01
$\Delta E_e[\Delta E_e(BSSE)]$	−12.02(−9.60)	−8.92(−6.88)	−8.25(−6.23)	−6.74(−4.81)	−6.71(−4.47)	−5.64(−3.90)
			avtz			
$A-W_a$	−2.68(−2.33)	−2.73(−2.39)		−3.16(−2.71)		−3.01(−2.57)
$A-W_b$	−2.89(−2.46)	−1.05(−0.80)		−3.16(−2.71)		−3.01(−2.57)
W_a-W_b	−5.10(−4.63)	−5.02(−4.61)		0.12(0.12)		0.16(0.17)
total two body	−10.67(−9.43)	−8.80(−7.80)		−6.20(−5.31)		−5.86(−4.97)
A−W−W	−1.09(−1.14)	0.44(0.41)		0.37(0.36)		0.35(0.34)
relaxation	0.20	0.04		0.03		0.02
$\Delta E_e[\Delta E_e(BSSE)]$	−11.57(−10.37)	−8.31(−7.34)		−5.79(−4.91)		−5.50(−4.61)

[a] BSSE-corrected values are shown in parentheses. [a] m(minimum) and sp(saddle point), Figure 2.

The two lowest minima AW_2_m1 and AW_2_m2 (Figures 2a, 2b) are cyclic trimers of C_1 and C_s symmetry, respectively, in which the acetylene molecule acts simultaneously as a proton donor and a proton acceptor to neighboring water molecules. In essence, both structures can be viewed as resulting from the interaction of a water dimer (albeit with different orientation) with A. The difference between m1 and m2 lies in the orientation of the T- and Y-water molecules (cf. Figure 2). In the former, the water molecules are simultaneously proton donors and proton acceptors to A, whereas in the latter, the T-water is a double H donor and the Y-water a double H acceptor.

The van der Waals (vdW) $H_1...O_a$ distance in AW_2_m1 is increased by ∼0.02 Å and the $C_2C_1O_1$ angle (151.9°) is decreased by 27.6° with respect to the AW−Y minimum (Figure 1)[1] at the MP2/avtz level. The intermolecular distance between the two water molecules, $O_b...H_{1a}$, is 1.916 Å, 0.017 Å shorter than the corresponding value in the water dimer (W_2),[15b] and the angle $H_{1a}-O_a...O_b$ is 13.6° as contrasted to 5.7° in W_2.[15c] In general, the structure of the water dimer fragment within the AW_2_m1 minimum is very similar to that of the free W_2.[15b,c] In contrast, the vdW distances in m2 are 0.1−0.3 Å longer than the corresponding distances in m1, mainly because the T-water in m1 acts as double H donor in that configuration.

The MP2 interaction energies $\Delta E_e[\Delta E_e(BSSE)]$ for the global minimum (AW_2_m1) with the avdz and avtz sets are −12.02[−9.60] and −11.57[−10.37] kcal/mol, respectively. Upon corrections for ZPE, these become $\Delta E_0(BSSE) = -5.76$ (avdz) and −6.70 (avtz) kcal/mol. The corresponding $\Delta E_e[\Delta E_e(BSSE)]$ $\{\Delta E_0(BSSE)\}$ energies for (AW_2_m2) are −8.92[−6.88] {−3.71} kcal/mol with the avdz and −8.31[−7.34]{−4.37} kcal/mol with the avtz sets, respectively. Dykstra[7] previously reported ΔE_e (ΔE_0) values of −12.65 (−8.17) kcal/mol for the AW_2 (cyclic) cluster using the MMC approach but without referring to any specific geometry. The energetic stabilization of m1 with respect to m2 by ∼2.3 kcal/mol (MP2/avtz) is also reflected in the more "open" structure of the latter when compared to the former. From Table 4, it is seen that a large portion (∼74%) of this difference arises from the $A-W_b$ interaction, which is weaker by 1.7 kcal/mol (MP2/avtz, see Table 4) in m2. Furthermore, there is a 1.55 kcal/mol difference between the two minima in the three-body term $A-W_a-W_b$ which is attractive (−1.14 kcal/mol) for m1 but repulsive (+0.41 kcal/mol) for m2. This is consistent with the "homodromic" topology of the ring in m1 and the fact that these networks have been previously reported[14c] to exhibit larger nonadditivities than other hydrogen bonding arrangements. The two-body (W_a-W_b) term is nearly identical in the two isomers (−4.63 vs −4.61 kcal/mol, MP2/avtz, BSSE-corrected) and to the free water dimer interaction (−4.71 kcal/mol, Table 1), indicating that an almost unperturbed water dimer exists within the cluster, a fact that is also evident by the intermolecular W−W separations discussed previously.

The geometries of the third and the fourth minima AW_2_m3 and AW_2_m4 (both of C_{2h} symmetry) are shown in parts d and f of Figure 2. In m3, two equivalent (AW−Y) bonds are formed, whereas in m4, two equivalent (AW−T) bonds are formed. When compared to the AW−Y and AW−T structures,[1] both the Y- and T-vdW bond distances in m3 and m4 minima increase by approximately 0.04 Å. Practically, the geometries of A and W molecules within the m3 and m4 clusters are identical with those of AW−Y and AW-T structures, respectively.

With regard to the MP2/avtz interaction energies $\Delta E_e[\Delta E_e(BSSE)]$ of m3 and m4, these are −5.79[−4.91] and −5.50 [−4.61] kcal/mol, respectively (cf. Table 4). As expected, these are almost twice as large as the corresponding $\Delta E_e(BSSE)$ values of the AW−Y and AW−T isomers, viz. −2.72 × 2 and −2.56 × 2 kcal/mol,[1] a result consistent with the fact that the rest of the terms in the many-body expansion (two-body W_a-W_b < 0.2 kcal/mol and three-body $A-W_a-W_b$ < 0.4 kcal/mol) are quite small and repulsive. These terms are responsible for the destabilization of m3 and m4 with respect to the global minimum (m1), although the former two have slightly larger two-body $A-W_a$ and $A-W_b$ terms with respect to m1 because of the more optimal orientation of the water molecules on either side of (A) when compared to the ring m1 structure. Inclusion of ZPE corrections produces $\Delta E_0(BSSE) = -3.03$ kcal/mol (m3) and −2.46 (m4) kcal/mol at the MP2/avtz level.

Finally, two saddle point structures, AW_2_sp1 and AW_2_sp2, both of C_s symmetry (see Figure 2c,e) were located. The sp1 is a second-order saddle point (two imaginary frequencies) constituting a three-member ring, whereas the sp2 is a transition state (one imaginary frequency) resulting from the m3 by a 90° rotation of the σ plane of one of the water molecules around the acetylene axis. The MP2/avdz interaction energies of sp1 and sp2, $\Delta E_e[\Delta E_e(BSSE)]$ $\{\Delta E_0(BSSE)\}$, are −8.25[−6.23] {−3.57} and −6.71[−4.47]{−2.47} kcal/mol, respectively. Judging from the variation of the energetics of the minima with

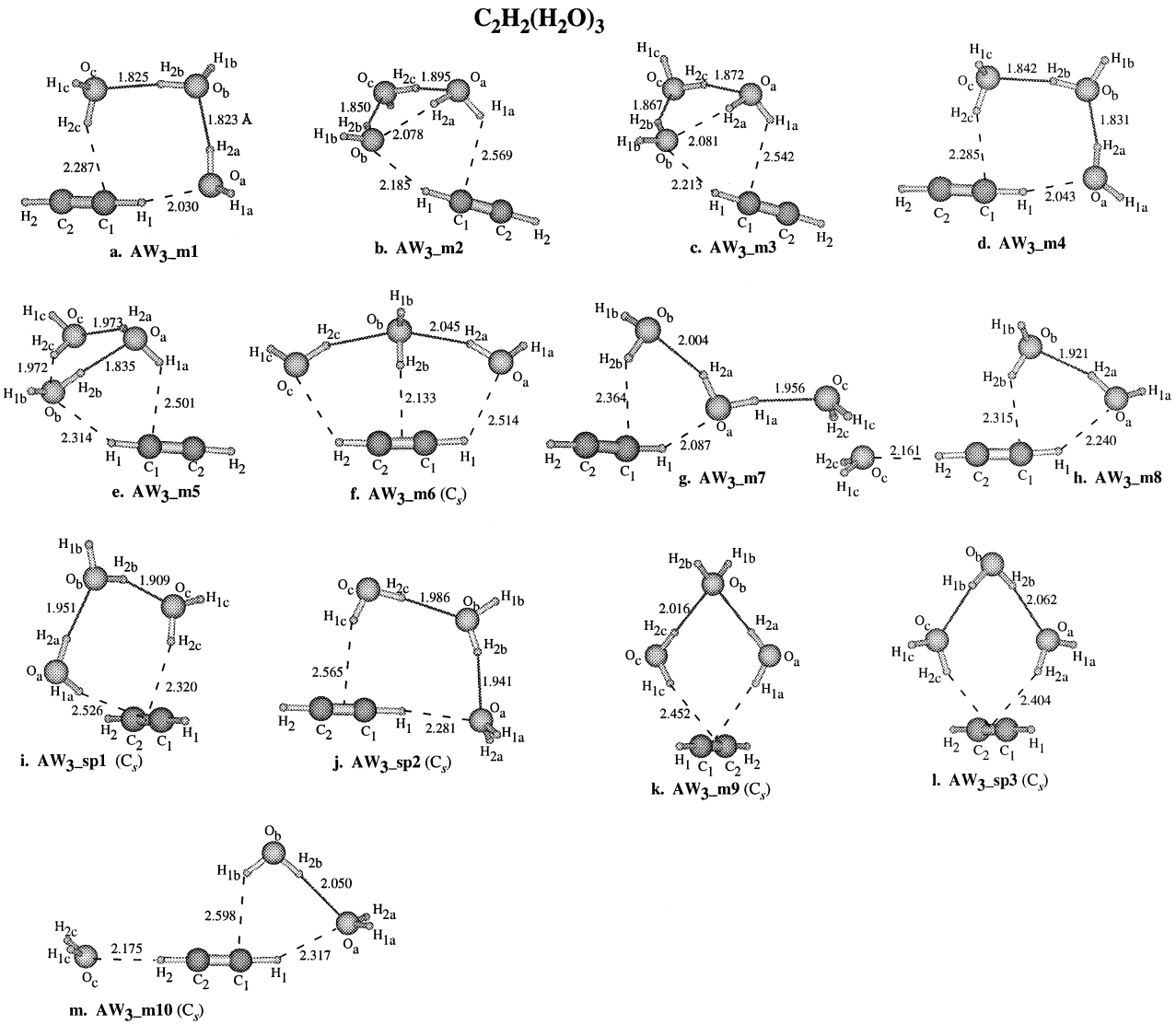

Figure 3. Geometries of the 10 minima (AW_3_ m*n*, $n = 1-10$) and the three saddle points (AW_3_sp*n*, $n = 1-3$) of AW_3. Bond distances in Å at the MP2/avdz level.

basis set, we estimate that these energies are ∼0.5 kcal/mol weaker than the analogous values with the avtz set.

c. C_2H_2 $(H_2O)_3$. We located 10 minima and 3 saddle points on the PES of AW_3. The optimal structures, together with representative intermolecular vdW distances, are shown in Figure 3. The depicted configurations were derived by combining the following sets of building units: $W_3 + A$, $W_2 + A + W$, $W_2 + AW$, $AW_2 + W$, $AW + 2W$, and $A + 3W$. All structures were fully optimized at the MP2/avdz level.[16c] Total energies (E_e) and interaction energies ΔE_e, ΔE_e(BSSE), and ΔE_0 (BSSE) are listed in Table 5; the vibrational frequencies and the IR intensities of the global minimum (m1) are given in Table 3.[16d] Finally, the decomposition of interaction energies into two-, three- and four-body terms for 6 selected minima are presented in Table 6. The structures of the stationary points fall into groups according to the various hydrogen bonding networks that are formed and are discussed as such below.

The AW_3_m1 and AW_3_m4 minima and the AW_3_sp2 saddle point (two imaginary frequencies) form a four member heavy atom ring (see Figure 3 parts a, d, and j). The global (m1) minimum resembles the W_4 cyclic tetramer[15] arrangement but with one W replaced by the C−H bond of A. The m1 and m4 isomers are quite similar, with the main difference being the relative positions of the hydrogens H_{1a} and H_{1b} with respect to the almost planar $C_1O_aO_bO_c$ ring: H_{1a} is up and H_{1b} is down (ud) in m1, whereas H_{1a} is down and H_{1b} is up (du) in m4. In this notation, the W_3 moiety in m1 and m4 can be characterized as udu and duu, respectively. A noted difference between (m1, m4) and sp2 is that, in the former, every water acts as a donor−

TABLE 5: Total Energies E_e (hartree), Interaction Energies ΔE_e (kcal/mol), Corrected for BSSE [ΔE_e(BSSE)], and Zero-Point Energy [ΔE_0(BSSE)] for AW_3 at the MP2/avdz Level of Theory

AW_3 [a]	E_e	ΔE_e	ΔE_e(BSSE)	ΔE_0(BSSE)
m1	−305.910717	−21.96	−17.80	−11.46
m2	−305.909968	−21.49	−17.54	−11.09
m3	−305.909879	−21.43	−17.47	−11.05
m4	−305.909764	−21.36	−17.25	−11.07
m5	−305.909479	−21.18	−17.12	−10.63
m6	−305.903302	−17.30	−13.81	−8.47
m7	−305.902655	−16.90	−13.55	−8.10
m8	−305.901287	−16.04	−12.60	−7.65
sp1[b]	−305.901011	−15.87	−12.43	−7.79
sp2[c]	−305.899517	−14.93	−11.55	−6.66
m9	−305.898487	−14.28	−10.92	−5.91
sp3[b]	−305.896882	−13.28	−10.11	−5.80
m10	−305.895900	−12.66	−9.62	−5.35

[a] m(minimum) and sp(saddle point), Figure 3. [b] Three imaginary frequencies. [c] Two imaginary frequencies.

TABLE 6: Many-Body Decomposition of the Interaction Energies (kcal/mol) for the m1, m2, m5, m6, m7, and m9 Minima of AW_3 at the MP2/avdz Level of Theory[a]

AW_3 [b]	m1	m2	m5	m6	m7	m9
$A-W_a$	−3.29(−2.19)	−1.27(−0.59)	−2.54(−1.82)	−2.49(−1.99)	−3.02(−2.08)	−2.99(−2.21)
$A-W_b$	−1.18(−1.03)	−3.07(−2.25)	−2.92(−2.22)	−2.62(−1.54)	−2.91(−2.09)	0.25(0.30)
$A-W_c$	−2.94(−1.95)	−1.03(−0.87)	0.34(0.52)	−2.49(−1.99)	−0.29(−0.24)	−2.99(−2.21)
W_a-W_b	−5.14(−4.14)	−4.60(−3.91)	−4.87(−3.82)	−4.82(−4.02)	−5.12(−4.33)	−5.18(−4.45)
W_a-W_c	−1.25(−1.15)	−4.43(−3.50)	−4.67(−3.87)	0.47(0.49)	−5.29(−4.48)	1.13(1.31)
W_b-W_c	−5.14(−4.13)	−4.92(−3.96)	−4.60(−3.79)	−4.82(−4.02)	0.48(0.49)	−5.18(−4.44)
total two body	−18.94(−14.60)	−19.32(−15.08)	−19.25(−15.00)	−16.78(−13.07)	−16.52(−12.73)	−14.96(−11.70)
$A-W_a-W_b$	−0.72(−0.81)	0.26(0.20)	−0.90(−0.94)	−0.74(−0.83)	−1.02(−1.15)	0.31(0.29)
$A-W_a-W_c$	−0.55(−0.60)	−0.17(−0.22)	0.33(0.30)	0.23(0.21)	−0.45(−0.45)	−0.14(−0.04)
$A-W_b-W_c$	−0.64(−0.70)	−0.49(−0.55)	0.26(0.27)	−0.74(−0.83)	0.05(0.04)	0.31(0.29)
$W_a-W_b-W_c$	−1.20(−1.25)	−2.17(−2.33)	−2.13(−2.28)	0.37(0.31)	0.47(0.50)	0.23(0.28)
total three body	−3.11(−3.36)	−2.57(−2.91)	−2.44(−2.66)	−0.87(−1.14)	−0.95(−1.05)	0.71(0.81)
$A-W_a-W_b-W_c$	−0.33(−0.27)	−0.04(0.01)	0.06(0.08)	0.01(0.07)	−0.03(0)	−0.07(−0.06)
relaxation	0.43	0.44	0.46	0.34	0.23	0.04
$\Delta E_e[\Delta E_e(BSSE)]$	−21.96(−17.80)	−21.49(−17.54)	−21.18(−17.12)	−17.30(−13.81)	−16.90(−13.55)	−14.28(−10.92)

[a] BSSE-corrected values are shown in parentheses. [b] m1 to m9 minima as shown in Figure 3.

acceptor to nearest neighbors, whereas in the latter, the W_c and W_a fragments are double H-donors and double acceptors, respectively.

The interaction energies $\Delta E_e[\Delta E_e(BSSE)]\{\Delta E_0(BSSE)\}$ are −21.96[−17.80]{−11.46}, −21.36[−17.25]{−11.07}, and −14.93[−11.55]{−6.66} kcal/mol for m1, m4, and sp2, respectively. It is interesting to point out that the ΔE_0(BSSE) interaction energies for the m2, m3, and m4 minima are almost identical (−11.09, −11.05, and −11.07 kcal/mol, cf. Table 5). The many-body analysis of the global minimum (m1) configuration, listed in Table 6, shows that (BSSE-corrected) total two-, three-, and four-body terms are −14.60, −3.36, and −0.27 kcal/mol, respectively, summing up to −18.23 kcal/mol, yielding a ΔE_e(BSSE) of −17.80 kcal/mol when the total relaxation energy of +0.43 kcal/mol is taken into account. Furthermore, we obtain an interaction of A with the three water molecules of −9.56 (−7.46 including ZPE) kcal/mol by summing together the two-body terms $A-W_i$, the three-body terms $A-W_i-W_j$, the 4-body term $A-W_a-W_b-W_c$, and the relaxation energy.

The AW_3_m2, AW_3_m3, and AW_3_m5 minima all have a cyclic water trimer structure that interacts with A via two vdW bonds (Figure 3 parts b, c, and e). The dihedral angles between the planes $C_1O_bO_a$ and $O_bO_aO_c$ are 108.5°, 107.4°, and 96.3° for m2, m3, and m5, respectively. The directions of the hydrogen-bonded H atoms within the W_3 fragment are, for a fixed orientation of A with respect to W_3, clockwise (m2 and m3) and counterclockwise (m5). The main difference between the m2 and m3 isomers lies in the direction of the free H-atom of the W_c fragment which is "down" for m2 and "up" for m3, with respect to the $O_aO_bO_c$ plane; the direction of the rest of the "free" H atoms for W_a and W_b being the same.

The interaction energies $\Delta E_e[\Delta E_e(BSSE)]\{\Delta E_0(BSSE)\}$ are −21.49[−17.54]{−11.09}, −21.43[−17.47]{−11.05}, and −21.18[−17.12]{−10.63} kcal/mol for m2, m3, and m5, respectively. We note that the BSSE-corrected interaction energies of the five minima (m1−m5) discussed so far are within an energy range of 0.68 kcal/mol (0.83 kcal/mol with ZPE corrections). The many-body analysis of the configurations of the m2 and m5 minima (the m3 being very similar to m2), shown in Table 6, indicates that the BSSE-corrected total contributions of the two-, three- and four-body terms are −15.08, −2.91, ∼0.0 kcal/mol (for m2) and −15.0, −2.66, +0.1 kcal/mol (for m5). The corresponding relaxation terms are similar (+0.44 and +0.46 kcal/mol respectively for m2 and m5). At the m2 and m5 minimum configurations, the interaction of A with the three water molecules is −5.78 (−4.24 including ZPE) kcal/mol (m2) and −5.34 (−3.78) kcal/mol (m5), values that are about half of the analogous interaction in m1. As expected, the water-only ($W_a-W_b-W_c$) three-body term is larger for m2 and m5 than for m1 because of the formation of the water trimer ring in the first two. However, the total four-body term for m1 is larger than for m2 because of the formation of the homodromic four heavy-atom ring in the former, again in accordance with previous conclusions[14c] suggesting the maximization of the nonadditivities for homodromic hydrogen-bonding networks.

The AW_3_m6 minimum (Figure 3f) is the first minimum of higher symmetry (C_s) found. The five heavy atoms form a pentagonal structure of trapezoidal topology divided in two equal parts by the $H_{2b}...\equiv$ (middle of the A-triple bond) line. Its interaction energy $\Delta E_e[\Delta E_e(BSSE)]\{\Delta E_0(BSSE)\}$ is −17.30[−13.81]{−8.47} kcal/mol, placing it 4.0 kcal/mol (3.0 when ZPE corrections are included) above the global minimum. The total (BSSE-corrected) two-, three- and four-body interactions, listed in Table 6, are −13.07, −1.14, and +0.1 kcal/mol, respectively, showing the dominance of the two-body contributions. The interaction of A with the three water molecules is −8.67 (−6.73 including ZPE) kcal/mol.

The AW_3_m7 minimum originates from the interaction of AW_2_m1 with a water molecule via a $H_{1a}...O_c$ vdW bond (Figure 2g), whereas the AW_3_m8 and AW_3_m10 minima (the second of C_s symmetry) are reminiscent of the AW_2_m1 and AW_2_m2 configurations interacting with a water molecule via a $H_2...O_c$ (Y-like) vdW bond (Figure 3h,m). The interaction energies $\Delta E_e[\Delta E_e(BSSE)]\{\Delta E_0(BSSE)\}$ are −16.90[−13.55]{−8.10}, −16.04[−12.60]{−7.65}, and −12.66[−9.62]{−5.35} kcal/mol for m7, m8, and m10, respectively. By summing up the interaction energies of AW_2_m1 and AW−Y,[1] we obtain ΔE_e(BSSE) = −9.60−2.62 = −12.22 kcal/mol, just 0.4 kcal/mol (0.3 kcal/mol including ZPE) weaker than ΔE_e(BSSE) of AW_3_m8 (Table 5), rationalizing our previous characterization of the m8 minimum as the combination of the interaction between the AW_2_m1 moiety and a water molecule in the Y arrangement. The same holds for AW_3_m10, for which the corresponding difference is just 0.12 kcal/mol (0.05 kcal/mol including ZPE). The analysis of the many-body energy terms for selected AW_3 minima suggests that the nonadditive (three-body and higher) terms are larger for the global minimum (m1) for which they amount to 18%, again in accordance with the formation of the homodromic ring incorporating all fragments. The percentage contribution of the many-body terms decreases with increasing separation from the global minimum, becoming 6% for m7.

The last group of the AW_3 isomers is composed of the AW_3_m9 minimum, and the third order (3 imaginary frequencies) saddle structures, AW_3_sp1 and AW_3_sp3 (Figure 3 parts k, i, and l). All three have C_s symmetry and four member rings $O_aO_bO_c\equiv$, where $\equiv$ represents the center of the acetylene triple bond. Their energetics, $\Delta E_e[\Delta E_e(\text{BSSE})]\{\Delta E_0(\text{BSSE})\}$, are −14.28[−10.92]{−5.91}, −15.87[−12.43]{−7.79}, and −13.28[−10.11]{−5.80} kcal/mol for m9, sp1, and sp3, respectively. The total three-body interaction for m9 is positive (+0.8 kcal/mol, Table 6), notably the only destabilizing three-body interaction in all 10 AW_3_m configurations studied.

d. C_2H_2 $(H_2O)_4$. For the AW_4 cluster, we located 30 minima (AW_4_m1 to AW_4_m30) and three saddle point structures (AW_4_sp1, 2, 3) which are depicted in Figure 4. With the exception of the m19, m26, and m27 minima and sp1 and sp2 saddle points, which are obtained at the MP2/4-31G level,[16e] all other structures were fully optimized at the MP2/avdz level of theory.[16e] Out of the 30 minima studied, only two (m28 and m30) belong to the S_2 and C_{2h} point groups, whereas the rest lack any symmetry elements (C_1). The minima were obtained by considering the following building units: W + A, W_3 + W + A, W_3 + AW, W_2 + AW_2, $2W_2$ + A, W_2 + 2W + A, 4W + A, AW_3 + W, AW_2 + 2W, and AW + 3W. The total and interaction energies are listed in Table 7, whereas the many-body analysis for eight selected minima is presented in Table 8. The harmonic vibrational frequencies and IR intensities for m1 are listed in Table 3, whereas corresponding values for m8 and m9 are available in the Supporting Information.[16f] Because ZPE corrections have been computed only for the m1, m8, and m9 minima, the main body of the interaction energy analysis is based on ΔE_e and ΔE_e(BSSE) values. Below, we discuss the different structures according to their grouping into similar morphologies.

The AW_4_m1, AW_4_m4, AW_4_m6, and AW_4_m7 minima span an energy difference range of 1 kcal/mol and are composed of a cyclic water tetramer (W_4) interacting with the A moiety via two adjacent W molecules. In all four previous structures, the four-member oxygen rings ($O_aO_bO_cO_d$) are almost planar with the A molecule located on the $O_aO_bC_1$ plane, with the dihedral angles between these two planes ranging from 111 (m1) to 91° (m7). Within (m1 and m4) and (m6 and m7), the W_4 fragment assumes the structure of the free W_4 global (udud) and first local (uudd) minima, respectively, according to the MP2/avdz//CCSD(T) and MP2−R12 calculations of Schultz et al.[17] These four minima result from all possible combinations of the direction of the "hydrogen-bonded" H atoms in the W_4 ring with respect to a fixed A orientation (clockwise, counterclockwise) and the position of the "free" H-atoms with respect to the $O_aO_bO_cO_d$ plane, viz., (udud) and (uudd).

The interaction energies $\Delta E_e[\Delta E_e(\text{BSSE})]$ are −33.89[−28.01], −33.51[−27.57], −33.08[−27.25], and −32.96[−26.96] kcal/mol for m1, m4, m6, and m7, respectively (cf. Table 7). When ZPE corrections are included, the interaction energy ΔE_0(BSSE) of m1 becomes −18.67 kcal/mol. At the same level of theory (MP2/avdz), the free water tetramer W_4 has an interaction energy $\Delta E_0(\text{BSSE}) = 16.03$ kcal/mol.[15] Therefore, the difference of −2.64 kcal/mol closely resembles the binding of AW_4_m1 with respect to W_4 + A. This value is practically equal to the sum of ΔE_0(BSSE) interactions for AW−T + AW−Y (−2.59 kcal/mol).[1] The analysis of many-body energy terms for m1 (cf. Table 8), reveals that the sum of two-, three-, four-, and five-body interactions are −21.90, −6.65, −0.51, and +0.01 kcal/mol, respectively, with the total relaxation R being +1.03 kcal/mol.

The AW_4_m2, AW_4_m3, and AW_4_m5 minima are also composed of water tetramers, but with two diagonal water molecules of the W_4 ring interacting with A through two vdW bonds, forming puckered four-member rings with dihedral angles between the $O_aO_bO_d$ and $O_bO_cO_d$ planes of 150.4°, 150.6°, and 155.0°, respectively (see Figure 4 parts b, c, and e). As with the previous group, these minima arise from the different choices of the direction of the "hydrogen-bonded" (clockwise, counterclockwise) and "free" (up, down, and planar (p)) H atoms. Although the m2 and m3 minima are practically degenerate, their energy difference being 0.11 kcal/mol (0.12 kcal/mol including BSSE), they correspond to structures that have different directions as regards the "hydrogen-bonded" H atoms within the W_4 fragment (clockwise for m2 and counterclockwise for m3). It should be mentioned that the corresponding structures (dpud) and (ddup) of the gas-phase water tetramer W_4, lying ∼1.2 kcal/mol higher than the global minimum, are saddle points of second and first order on the water tetramer PES,[17] but are stabilized as minima m2 and m3 in AW_4. The corresponding interaction energies $\Delta E_e[\Delta E_e(\text{BSSE})]$ are −33.68[−27.47], −33.57[−27.35], and −33.46[−27.25] kcal/mol for m2, m3, and m5, see Table 7. Note that BSSE corrections alter the order of the minima to m4, m2, m3, and m5 = m6.

The AW_4_m8 and AW_4_m18 minima are formed by the interaction of a perturbed "cage" water tetramer with A (Figure 4 parts h and t). The cage W_4 structure was found to be a minimum on the PES of the ASP−P (anisotropic site potential neglecting all nonpairwise additive effects) potential by Gregory and Clary;[18] however, at the MP2/dzp level, the cage morphology was found to collapse to the global ring minimum.[18] In the W_4 cage, the H_{1a} hydrogen forms a vdW bond with the O_c atom, but in the m8 and m18 minima, this interaction is altered because of the intervention of the A molecule and the formation of two vdW bonds between W_4 and A. The difference between m8 and m18 lies again in the topology of the hydrogen bonding network. Furthermore, the W_4 ring is more "puckered" than the one in m2, m3, and m5 minima: the dihedral angles between the two oxygen planes $O_aO_bO_d$ and $O_bO_dO_c$ are 95.6° (m8) and 110.4° (m18).

The interaction energies $\Delta E_e[\Delta E_e(\text{BSSE})]$ are −30.81[−25.01] kcal/mol for m8 and −28.63[−23.01] kcal/mol for m18. Including ZPE corrections, the m8 interaction energy becomes −15.89 kcal/mol. The energy difference of 2.18 kcal/mol (2.0 kcal/mol including the BSSE) between the two isomers is rather due to the extra H bond in m8.

The AW_4_m9 minimum (Figure 4i) forms a cyclic pentamer ring that incorporates A and resembles the free W_5 duduu configuration.[15] The replacement of any other water molecule by A collapses to the previous minimum. All six heavy atoms are approximately on the same plane and the interaction energy $\Delta E_e[\Delta E_e(\text{BSSE})]\{\Delta E_0(\text{BSSE})\}$ is −30.64[−25.14]{−16.57} kcal/mol. Correcting for BSSE and ZPE was found to invert the ordering between m8 and m9. As expected from the homodromic ring configuration of this structure, all nonadditive (three-body and higher) energy terms are negative; that is, they all stabilize this particular network.

The common feature among the AW_4_m10, AW_4_m16, and AW_4_m17 minima (Figure 4 parts j, p, and q) and the two first-order saddle point structures, AW_4_sp1 and AW_4_sp2 (Figure 4 parts r and s), is a water tetramer with identical topology, whose gas-phase configuration has symmetry C_s This structure was previously identified by Clementi et al.[19] and later discussed by Gregory and Clary.[18] The intervention of the A molecule destroys the C_s symmetry of the W_4 fragment in the m10, m16,

$C_2H_2(H_2O)_4$

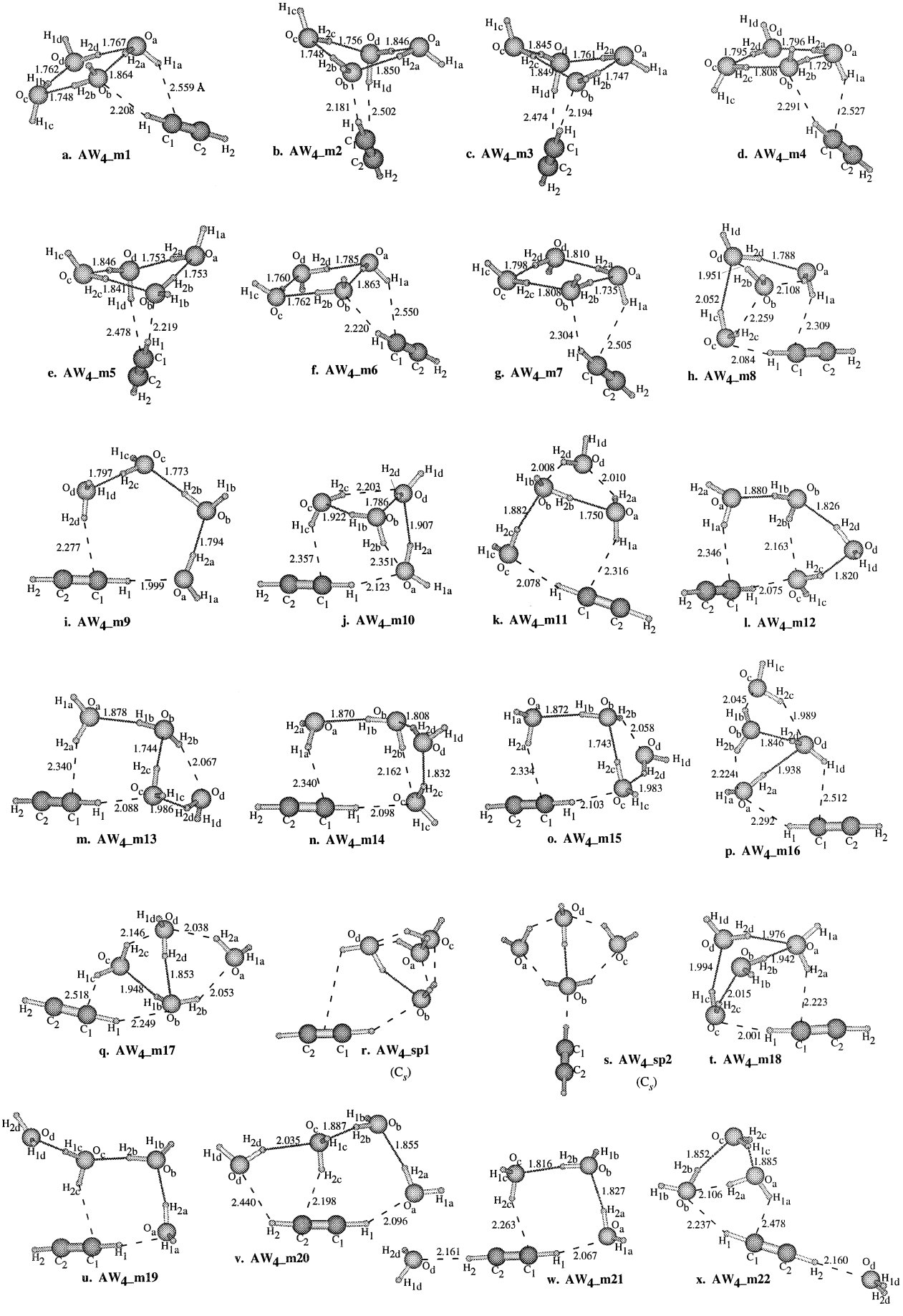
a. AW4_m1
b. AW4_m2
c. AW4_m3
d. AW4_m4
e. AW4_m5
f. AW4_m6
g. AW4_m7
h. AW4_m8
i. AW4_m9
j. AW4_m10
k. AW4_m11
l. AW4_m12
m. AW4_m13
n. AW4_m14
o. AW4_m15
p. AW4_m16
q. AW4_m17
r. AW4_sp1 (Cs)
s. AW4_sp2 (Cs)
t. AW4_m18
u. AW4_m19
v. AW4_m20
w. AW4_m21
x. AW4_m22

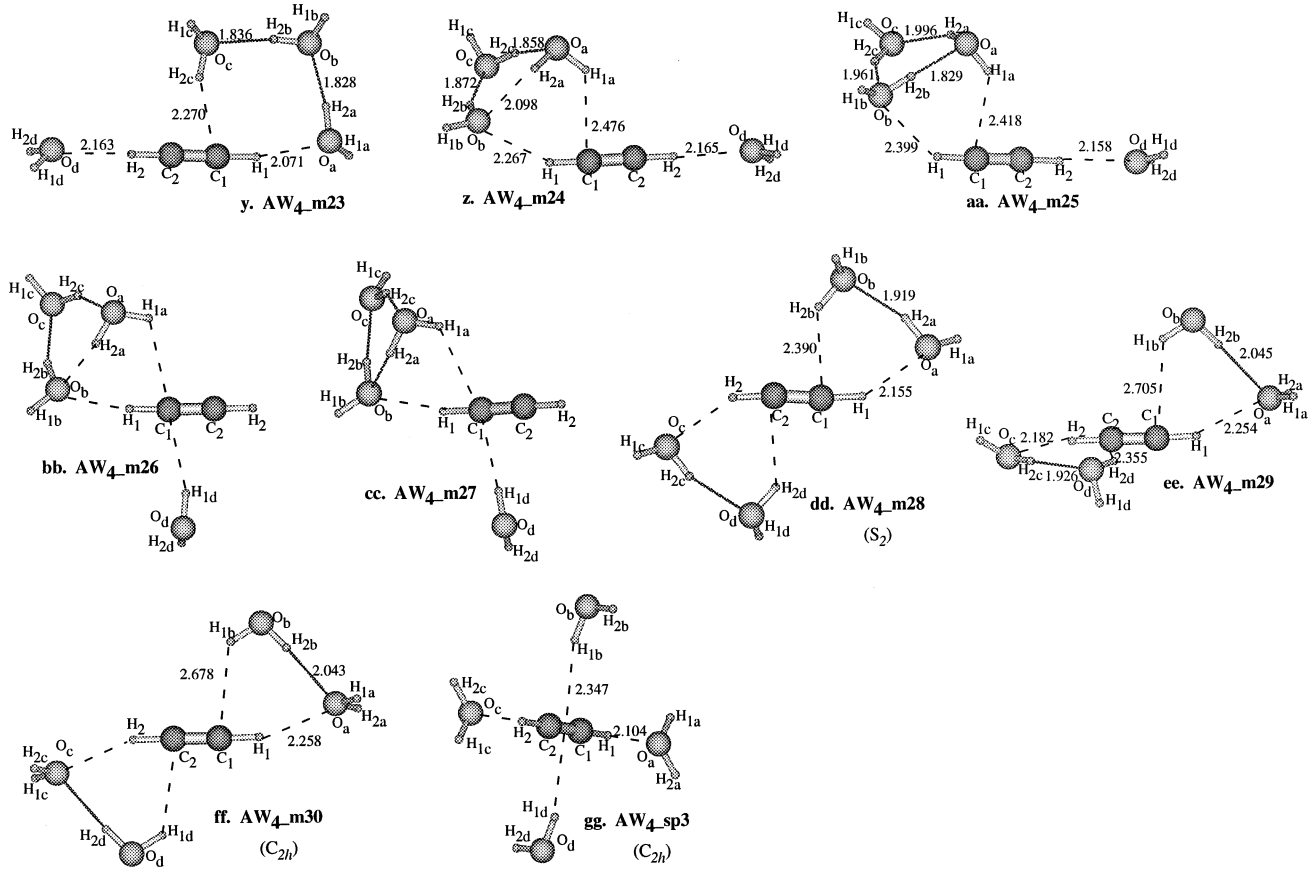

Figure 4. Geometries of the 30 minima (AW_4_m*n*, $n = 1-30$) and three saddle points (AW_4_sp*n*, $n = 1-3$) of AW_4 cluster. Bond distances in Å at the MP2/avdz level.

and m17 minima, but this symmetry is maintained in the sp1 and sp2 conformations. The difference between these five structures lies in which water molecule(s) of the W_4 fragment interacts with the acetylene. The dihedral angles between the oxygen planes $O_aO_bO_d$ and $O_bO_dO_c$ are 97.3°, 99.3°, and 115.3° in the m10, m16, and m17 minima, respectively.

The interaction energies $\Delta E_e[\Delta E_e(\text{BSSE})]$ are −30.63[−24.70], −28.78[−23.28], and −28.73[−23.27] kcal/mol for m10, m16, and m17, respectively; note that m16 and m17 are practically degenerate at this level of theory. The many-body analysis for the m10 isomer is given in Table 8. We remind the reader that the sp1 and sp2 structures were calculated at the MP2/4-31G level, and they might be lying higher than m17 and near to m18.

In the AW_4_m11 to AW_4_m15 series (Figure 4 parts k−o), a water trimer ring interacts with A through two vdW bonds forming an almost planar four member ring. The dihedral angles between the oxygen "triangles" and the "squares" range from 95 to 113°. It is interesting to note that all five minima lie within an energy range of 0.3 kcal/mol (with or without BSSE corrections) at the MP2/avdz level (Table 7). The five structures can be divided in three groups (m11), (m12 and m14), and (m13 and m15) according to the vdW bonds formed between the five molecules. The difference between m12 and m14, m13 and m15 is the H_{1d} hydrogen direction (up or down) with respect to the $O_bO_cO_d$ plane.

The AW_4_m19, AW_4_m20, AW_4_m21, and AW_4_m23 minima (Figure 4 parts u, v, w, and y) can be considered as AW_3_m1 + W_d and AW_3_m4 + W_d. The four-member rings $O_aO_bO_cC_1$ in m19, m21, and m23 are almost planar, but in m20, the dihedral angle between the $O_aO_bO_c$ and $O_bO_cC_1$ planes is −28.0°. The similarity between the m21 and m23 structures is

TABLE 7: Total Energies E_e (hartree), Interaction Energies ΔE_e (kcal/mol), Corrected for BSSE [ΔE_e(BSSE)], and Zero-Point Energy [ΔE_0(BSSE)] for AW_4 at the MP2/avdz Level of Theory

AW_4 [a]	E_e	ΔE_e	ΔE_e(BSSE)	ΔE_0(BSSE)
m1	−382.190641	−33.89	−28.01	−18.67
m2	−382.190305	−33.68	−27.47	
m3	−382.190136	−33.57	−27.35	
m4	−382.190037	−33.51	−27.57	
m5	−382.189952	−33.46	−27.25	
m6	−382.189348	−33.08	−27.25	
m7	−382.189163	−32.96	−26.96	
m8	−382.185732	−30.81	−25.01	−15.89
m9	−382.185459	−30.64	−25.14	−16.57
m10	−382.185443	−30.63	−24.70	
m11	−382.185102	−30.41	−24.65	
m12	−382.184782	−30.21	−24.52	
m13	−382.184743	−30.19	−24.49	
m14	−382.184703	−30.16	−24.41	
m15	−382.184659	−30.13	−24.36	
m16	−382.182504	−28.78	−23.28	
m17	−382.182414	−28.73	−23.27	
m18	−382.182267	−28.63	−23.01	
m20	−382.181013	−27.85	−22.52	
m21	−382.178107	−26.02	−20.82	
m22	−382.177154	−25.43	−20.41	
m23	−382.177139	−25.42	−20.28	
m24	−382.176850	−25.23	−20.26	
m25	−382.176520	−25.03	−19.95	
m28	−382.175652	−24.48	−19.60	
m29	−382.170289	−21.12	−16.58	
m30	−382.165349	−18.02	−13.87	
sp3 [b]	−382.161304	−15.48	−11.65	

[a] m(minimum) and sp(saddle point), Figure 4. [b] Four imaginary frequencies.

TABLE 8: Many-Body Decomposition of Interaction Energies ΔE_e (kcal/mol) of the m1, m2, m3, m4, m8, m9, m10, and m11 Minima of AW_4 at the MP2/avdz Level of Theory[a]

AW_4 [b]	m1	m2	m3	m4	m8	m9	m10	m11
$A-W_a$	−1.05(−0.37)	0.29(0.56)	−1.36(−1.14)	−2.71(−2.02)	−2.57(−1.66)	−3.34(−2.19)	−3.44(−2.45)	−2.88(−1.95)
$A-W_b$	−2.95(−2.20)	−3.22(−2.32)	−3.29(−2.40)	−2.88(−2.17)	−0.26(−0.18)	−0.72(−0.64)	−0.33(−0.17)	−1.10(−0.96)
$A-W_c$	−0.67(−0.58)	−1.17(−0.97)	0.44(0.70)	0.23(0.38)	−3.16(−2.12)	−0.70(−0.60)	−2.52(−1.65)	−3.37(−2.32)
$A-W_d$	−0.30(−0.24)	−2.34(−1.61)	−2.28(−1.51)	0.17(0.24)	−0.96(−0.84)	−2.88(−1.85)	−0.40(−0.30)	0.10(0.17)
W_a-W_b	−4.99(−4.07)	−4.88(−3.97)	−4.60(−3.48)	−4.74(−3.59)	−4.65(−4.00)	−5.00(−3.95)	−3.76(−3.26)	−4.66(−3.53)
W_a-W_c	−1.75(−1.59)	−1.85(−1.69)	−1.90(−1.73)	−1.69(−1.52)	−0.82(−0.61)	−1.03(−0.96)	0.10(0.27)	−1.07(−0.95)
W_a-W_d	−4.87(−3.78)	−4.23(−3.25)	−4.37(−3.25)	−4.84(−3.81)	−4.82(−3.73)	−0.80(−0.74)	−4.50(−3.63)	−4.75(−4.00)
W_b-W_c	−4.84(−3.73)	−4.44(−3.32)	−4.53(−3.59)	−5.06(−4.05)	−1.92(−1.38)	−4.90(−3.81)	−3.91(−3.02)	−5.25(−4.36)
W_b-W_d	−1.71(−1.57)	−2.09(−1.88)	−2.08(−1.87)	−1.68(−1.54)	−4.41(−3.57)	−0.94(−0.86)	−4.51(−3.34)	−4.57(−3.81)
W_c-W_d	−4.85(−3.76)	−4.68(−3.55)	−4.63(−3.67)	−5.04(−4.00)	−4.40(−3.71)	−4.98(−3.94)	−4.49(−3.92)	0.54(0.69)
total two body	−27.99(−21.90)	−28.63(−22.00)	−28.59(−21.94)	−28.25(−22.08)	−27.98(−21.81)	−25.28(−19.56)	−27.77(−21.47)	−27.01(−21.01)
$A-W_a-W_b$	0.50(0.46)	0.51(0.47)	−0.68(−0.75)	−1.09(−1.16)	0.27(0.26)	−0.73(−0.80)	0.19(0.14)	−0.61(−0.62)
$A-W_a-W_c$	0.03(0.02)	0.02(0.06)	0.02(0.06)	0.13(0.11)	−0.39(−0.49)	−0.18(−0.20)	−0.24(−0.32)	−0.46(−0.52)
$A-W_a-W_d$	−0.32(−0.29)	0.50(0.43)	−0.46(−0.52)	0.28(0.27)	−0.51(−0.53)	−0.43(−0.46)	−0.38(−0.40)	0.34(0.32)
$A-W_b-W_c$	−0.59(−0.61)	−0.53(−0.60)	0.51(0.47)	0.34(0.34)	−0.19(−0.22)	−0.15(−0.18)	−0.25(−0.30)	−0.61(−0.70)
$A-W_b-W_d$	0.00(0.00)	−0.21(−0.27)	−0.18(−0.24)	0.05(0.07)	−0.02(0.00)	−0.14(−0.15)	0.02(−0.01)	0.02(0.05)
$A-W_c-W_d$	−0.10(−0.12)	−0.53(−0.59)	0.55(0.49)	0.11(0.09)	−0.51(−0.58)	−0.59(−0.63)	0.19(0.17)	0.10(0.08)
$W_a-W_b-W_c$	−1.38(−1.46)	−1.42(−1.49)	−1.19(−1.28)	−1.50(−1.55)	0.34(0.32)	−1.30(−1.34)	0.42(0.35)	−1.17(−0.18)
$W_a-W_b-W_d$	−1.35(−1.43)	−1.04(−1.14)	−1.66(−1.74)	−1.47(−1.53)	−1.97(−2.13)	−0.23(−0.25)	−1.76(−1.85)	−2.20(−2.35)
$W_a-W_c-W_d$	−1.53(−1.60)	−1.20(−1.28)	−1.44(−1.50)	−1.38(−1.46)	−0.85(−0.94)	−0.27(−0.28)	0.30(0.31)	0.16(0.15)
$W_b-W_c-W_d$	−1.54(−1.62)	−1.66(−1.74)	−1.03(−1.12)	−1.36(−1.44)	0.47(0.43)	−1.26(−1.29)	−1.96(−2.07)	0.44(0.44)
Total three body	−6.27(−6.65)	−5.57(−6.14)	−5.55(−6.14)	−5.89(−6.26)	−3.36(−3.88)	−5.27(−5.57)	−3.47(−3.96)	−4.00(−4.34)
$A-W_a-W_b-W_c$	0.00(0.06)	0.05(0.06)	0.03(0.04)	−0.01(0.04)	−0.01(0.02)	−0.18(−0.15)	−0.07(−0.04)	−0.28(−0.23)
$A-W_a-W_b-W_d$	0.02(0.04)	0.08(0.12)	−0.18(−0.13)	0.00(0.05)	−0.01(0.03)	−0.12(−0.10)	−0.04(0.00)	0.00(0.05)
$A-W_a-W_c-W_d$	−0.05(−0.04)	0.02(0.04)	0.04(0.05)	0.02(0.04)	−0.22(−0.15)	−0.11(−0.10)	−0.04(−0.03)	0.02(0.04)
$A-W_b-W_c-W_d$	−0.07(−0.04)	−0.20(−0.16)	0.11(0.12)	0.05(0.03)	−0.2(0.00)	−0.13(−0.12)	−0.03(0.02)	0.04(0.03)
$W_a-W_b-W_c-W_d$	−0.61(−0.53)	−0.51(−0.44)	−0.51(−0.44)	−0.59(−0.50)	0.04(0.07)	−0.19(−0.18)	0.07(0.09)	0.00(0.04)
total four body	−0.71(−0.51)	−0.57(−0.38)	−0.52(−0.36)	−0.53(−0.34)	−0.22(−0.03)	−0.72(−0.65)	−0.11(0.04)	−0.21(−0.06)
$A-W_a-W_b-W_c-W_d$	0.06(0.01)	0.05(0.03)	0.04(0.03)	0.05(0.01)	0.04(0.00)	−0.04(−0.04)	0.01(−0.01)	0.06(0.01)
relaxation	1.03	1.03	1.05	1.11	0.72	0.68	0.71	0.75
$\Delta E_e[\Delta E_e$ (BSSE)]	−33.89(−28.01)	−33.68(−27.47)	−33.57(−27.35)	−33.51(−27.57)	−30.81(−25.01)	−30.64(−25.14)	−30.63(−24.70)	−30.41(−24.65)

[a] BSSE-corrected values are shown in parentheses. [b] All minimum structures are shown in Figure 4.

striking, and it is remarkable that these constitute separate minima (at least at the MP2/avdz level of theory), their difference being in the directions of the H_{1a} and H_{1b} hydrogen atoms with respect to the $O_aO_bO_c$ plane. Finally, the interaction energies $\Delta E_e[\Delta E_e(\text{BSSE})]$ are −27.85[−22.52], −26.02[−20.82], and −25.42[−20.28] kcal/mol for m20, m21, and m23, respectively. As expected, for m21(m23), these interaction energies are equal to the energies of AW_3_m1(m4) + AW−Y. Again note that the m19 isomer has been computed at the MP2/4-31G level of theory.

The AW_4_m22, AW_4_m24, and AW_4_m25 minima (Figure 4 parts x, z, and aa) can be viewed as the AW_3_m2, AW_3_m3, and AW_3_m5 structures, respectively, in which the A molecule is interacting with an additional water molecule in an Y arrangement (as an acceptor to acetylene). Correspondingly, the AW_4_m26 and AW_4_m27 isomers (obtained at the MP2/4-31G level) are seen as AW_3_m3 and AW_3_m2 isomers, respectively, interacting with a water molecule in a T fashion (Figures 4bb and 4cc). The first three minima lie within an energy range of 0.40 kcal/mol (0.46 kcal/mol including BSSE corrections), having interaction energies in the range −25.43 to −25.03 kcal/mol (−20.41 to −19.95 kcal/mol including BSSE corrections, cf. Table 7).

The AW_4_m28, AW_4_m29, and AW_4_m30 (Figure 4 parts dd, ee, and ff) are the energetically highest and most well separated minima studied in the present work, their energy differences being approximately 3 kcal/mol (Table 7). The m28 (S_2) and m30 (C_{2h}) minima can be thought of as "double" AW_2_m1 and AW_2_m2 configurations, whereas the m29 minimum can be thought of as a combination of the AW_2_m1 and AW_2_m2 structures. Although all of the heavy atoms in m30 and the four oxygen atoms in m28 are coplanar by symmetry, in the latter, all six heavy atoms are also, practically, coplanar. The interaction energies $\Delta E_e[\Delta E_e(\text{BSSE})]$ are −24.48[−19.60], −21.12[−16.58], and −18.02[−13.87] kcal/mol for m28, m29, and m30, respectively. By summing up twice the interaction energies of AW_2_m1 and AW_2_m2, we obtain −24.04[−19.20], −20.94[−16.48], and −17.84[−13.76] kcal/mol, values that are very close indeed to the interaction energies of m28, m29, and m30 minima.

Finally, the AW_4_sp3 (Figure 4gg) is a fourth order saddle point (four imaginary frequencies) of C_{2h} symmetry, and is composed of two independent Y and two independent T arrangements (Figure 1). Alternatively, it can be seen as a "superposition" of the AW_2_m3 and AW_2_m4 arrangements (Figure 2d,f). Its interaction energy $\Delta E_e[\Delta E_e(\text{BSSE})]$ is −15.48[−11.65] kcal/mol, as contrasted to the sum of interaction energies of two AW−Y and two AW-T isomers, which is −13.30[−9.56] kcal/mol.[1]

4. Summary

Extended parts of the multidimensional PESs of a number of acetylene−water, AW_x, $x = 2$, 3, and 4 clusters have been probed by ab initio calculations. Using chemical intuition and extended systematic searches on the multidimensional PESs with smaller basis sets to obtain candidates of stationary points, we have located 4, 10, and 30 minima for AW_2, AW_3, and AW_4 clusters, respectively. Although we cannot claim that every possible isomer has been located within the energy range considered here, we can ascertain that the global minima for these clusters have been identified. The energy separation between the located stationary points (minima and saddle points) is shown in Figure 5. As expected,[20] the density of the local

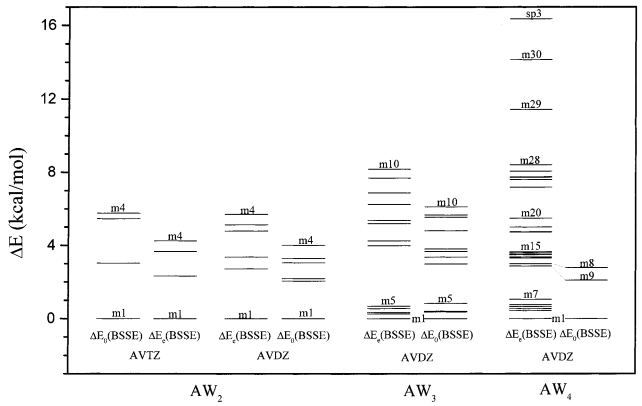

Figure 5. Interaction energies ΔE_e(BSSE) and ΔE_0(BSSE) of all stationary points of the AW_2, AW_3, and AW_4 clusters relative to the corresponding global minina (m1).

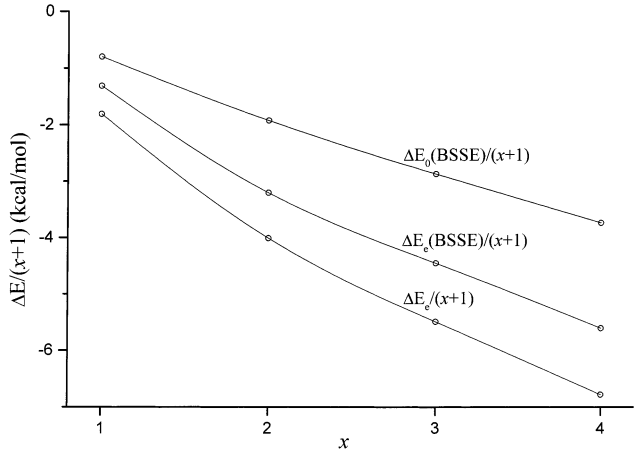

Figure 6. Variation of the "average" dissociation energies, $\Delta E_e/(x + 1)$, ΔE_e(BSSE)/$(x + 1)$, and ΔE_0(BSSE)/$(x + 1)$ of the global minima (m1) with cluster size x at the MP2/avdz level.

minima is increasing dramatically with cluster size, a manifestation of the energetic competition between different hydrogen bonding networks. For instance, for AW_4, the first 28 minima lie within a range of ~8 kcal/mol. To this end, corrections for BSSE and ZPE can alter the order of these closely spaced minima. Such is the case for the range of m10−m15 of AW_4 where six minima are packed within an energy range of just 0.34 kcal/mol and the change in order for m8 and m9 upon including ZPE corrections. The "average" interaction energies, $\Delta E_e/(x + 1)$, ΔE_e(BSSE)/$(x + 1)$, and ΔE_0(BSSE)/$(x + 1)$ for the AW, AW_2, AW_3, and AW_4 global mimima are plotted in Figure 6. The analysis of the many-body interactions for several hydrogen bonded networks indicates that there are different requirements as regards an empirical interaction potential needed to reproduce the relative cluster energetics: usually the low-(er) lying energy structures are stabilized because of the maximization of the nonadditive (mainly the three-body) components of the interaction energies, whereas higher lying structures are composed from mainly two-body interactions. Therefore, empirical interaction potentials that aim to reproduce the relative cluster energetics will need to include many-body effects because they need to describe both the ring configurations (large nonadditivities, mainly three-body) as well as other more compact configurations (mainly two-body) with the same accuracy.

Acknowledgment. Part of this work was performed under the auspices of the Division of Chemical Sciences, Office of Basic Energy Sciences, U.S. Department of Energy under Contract DE-AC06-76RLO 1830 with Battelle Memorial Institute, which operates the Pacific Northwest National Laboratory. Computer resources were provided by the Division of Chemical Sciences and by the Scientific Computing Staff, Office of Energy Research, at the National Energy Research Supercomputer Center (Berkeley, CA). D.T. acknowledges an Associated Western Universities (AWU) Fellowship during her visit to PNNL in the summer of 1998. This research was performed in the Environmental Molecular Sciences Laboratory, a national used facility funded by DOE's Office of Biological and Environmental Research.

Supporting Information Available: Optimal geometries of all AW_2 structures (Table 1). Harmonic vibrational frequencies and IR intensities of AW_2 stationary points (Table 2). Cartesian coordinates of all AW_3 structures (Table 3). Harmonic vibrational frequencies and IR intensities of AW_3 structures (Table 4). Cartesian coordinates of all AW_4 structures (Table 5). Harmonic vibrational frequencies and IR intensities of two AW_4 structures (Table 6). This material is available free of charge via the Internet at http://pubs.acs.org.

References and Notes

(1) Tzeli, D.; Mavridis, A.; Xantheas, S. S. *J. Chem. Phys.* **2000**, *112*, 6178.

(2) Tzeli, D.; Mavridis, A.; Xantheas, S. S. *Chem. Phys. Lett.* **2001**, *340*, 538.

(3) Engdahl, A.; Nelander, B. *Chem. Phys. Lett.* **1983**, *100*, 129.

(4) Peterson, K. J.; Klemperer, W. *J. Chem. Phys.* **1984**, *81*, 3842.

(5) Block, P. A.; Marshall, M. D.; Pedersen, L. G.; Miller, R. E. *J. Chem. Phys.* **1992**, *96*, 7321.

(6) Choi, S.-S.; Jung, K. W.; Jung, K.-H. *Int. J. Mass. Spectrosc. Ion Proc.* **1993**, *124*, 11.

(7) Dykstra, C. E. *J. Phys. Chem.* **1995**, *99*, 11680.

(8) van Voorhis, T.; Dykstra, C. E. *Mol. Phys.* **1996**, *87*, 931.

(9) (a) Dunning, T. H., Jr. *J. Chem. Phys.* **1989**, *90*, 1007. (b) Kendall, R. A.; Dunning, T. H., Jr.; Harrison, R. J. *J. Chem. Phys.* **1992**, *96*, 6796.

(10) Frisch, M. J.; Trucks, G. W.; Schlegel, H. B.; Scuseria, G. E.; Robb, M. A.; Cheeseman, J. R.; Zakrzewski, V. G.; Montgomery, J. A., Jr.; Stratmann, R. E.; Burant, J. C.; Dapprich, S.; Millam, J. M.; Daniels, A. D.; Kudin, K. N.; Strain, M. C.; Farkas, O.; Tomasi, J.; Barone, V.; Cossi, M.; Cammi, R.; Mennucci, B.; Pomelli, C.; Adamo, C.; Clifford, S.; Ochterski, J.; Petersson, G. A.; Ayala, P. Y.; Cui, Q.; Morokuma, K.; Malick, D. K.; Rabuck, A. D.; Raghavachari, K.; Foresman, J. B.; Cioslowski, J.; Ortiz, J. V.; Stefanov, B. B.; Liu, G.; Liashenko, A.; Piskorz, P.; Komaromi, I.; Gomperts, R.; Martin, R. L.; Fox, D. J.; Keith, T.; Al-Laham, M. A.; Peng, C. Y.; Nanayakkara, A.; Gonzalez, C.; Challacombe, M.; Gill, P. M. W.; Johnson, B. G.; Chen, W.; Wong, M. W.; Andres, J. L.; Head-Gordon, M.; Replogle, E. S.; Pople, J. A. *Gaussian 98*; Gaussian, Inc.: Pittsburgh, PA, 1998.

(11) (a) Boys, S. F.; Bernardi, F. *Mol. Phys.* **1970**, *19*, 553. (b) Davidson, E. R.; Chakravorty, S. J. *Chem. Phys. Lett.* **1994**, *217*, 48.

(12) (a) Van Duijneveldt, F. B.; van Duijneveldt-van de Rijdt, J. G. C. M.; van Lenthe, J. H. *Chem. Rev.* **1994**, *94*, 1873. (b) Jeziorski, B.; Moszynski, R.; Szalewicz, K. *Chem. Rev.* **1994**, *94*, 1887.

(13) Xantheas, S. S. *J. Chem. Phys.* **1996**, *104*, 8821.

(14) (a) Hankins, D.; Moskowitz, J. W.; Stillinger, F. H. *J. Chem. Phys.* **1970**, *53*, 4544. (b) Xantheas, S. S. *J. Chem. Phys.* **1994**, *100*, 7523. (c) Xantheas, S. S. *Chem. Phys.* **2000**, *258*, 225.

(15) (a) Xantheas, S. S.; Dunning, T. H., Jr. *J. Chem. Phys.* **1993**, *99*, 8774. (b) Xantheas, S. S. *J. Chem. Phys.* **1995**, *102*, 4505. (c) Xantheas, S. S.; Burnham, C. J.; Harrison, R. J. *J. Chem. Phys.* **2002**, *116*, 1493.

(16) Supporting Information. (a) Optimal geometries of all AW_2 structures are given in Table 1. (b) Harmonic vibrational frequencies and IR intensities of AW_2 stationary points are given in Table 2. (c) Cartesian coordinates of all AW_3 structures are given in Table 3. (d) Harmonic vibrational frequencies and IR intensities of AW_3 structures are given in Table 4. (e) Cartesian coordinates of all AW_4 structures are given in Table 5. (f) Harmonic vibrational frequencies and IR intensities of two AW_4 structures are given in Table 6.

(17) Schutz, M.; Klopper, W.; Luthi, H.-P.; Leutwyler, S. *J. Chem. Phys.* **1995**, *103*, 6114.

(18) Gregory, J. K.; Clary, D. C. *J. Phys. Chem.* **1996**, *100*, 18014.

(19) Kim, K. S.; Dupuis, M.; Lie, G. C.; Clementi, E.; *Chem. Phys. Lett.* **1986**, *131*, 451.

(20) Wales, D. J.; Scheraga, H. A. *Science* **1999**, *285*, 1368.